Dyes and Pigments 90 (2011) 275–283

Contents lists available at ScienceDirect

Dyes and Pigments

journal homepage: www.elsevier.com/locate/dyepig

Far-red absorbing squarylium dyes with terminally connected electron-accepting units for organic dye-sensitized solar cells

Takeshi Maeda [a,*], Hidekazu Nakao [b], Hisashi Kito [a], Hirokazu Ichinose [a], Shigeyuki Yagi [a], Hiroyuki Nakazumi [a,*]

[a] Department of Applied Chemistry, Graduate School of Engineering, Osaka Prefecture University, 1-1 Gakuen-cho, Naka-ku, Sakai, Osaka 599-8531, Japan
[b] Kobe Research, Nard Institute, Ltd., Kobe HIDEC, 3rd Floor, 6-7-4 Minatoshimaminami-cho, Chuo-ku, Kobe, Hyogo 650-0047, Japan

ARTICLE INFO

Article history:
Received 7 October 2010
Received in revised form
12 January 2011
Accepted 13 January 2011
Available online 20 January 2011

Keywords:
Squarylium dyes
Tetracyanoquinodimethane
Tetracyanoanthraquinodimethane
Metal-free
Dye-sensitized solar cells
Nanocrystalline TiO_2

ABSTRACT

Novel squarylium dyes with either terminally placed tetracyanoquinodimethane or tetracyanoanthraquinodimethane moieties as strong electron acceptors were designed and synthesized for use as sensitizers for TiO_2-based dye-sensitized solar cells (DSSCs). The photovoltaic performance of DSSCs indicates that two chromophores, strong electron acceptors and squarylium components, make independent contributions to photosensitization of nanocrystalline TiO_2. DSSCs fabricated from squarylium-based diads as sensitizers and chenodeoxycholic acid as the coadsorbent exhibited a high open-circuit voltage (up to 0.66 V), suggesting that the electron-accepting components showed some effect on electron injection from the squarylium chromophore to the conduction band of TiO_2. Under the coadsorbent-free conditions, the short-circuit photocurrent and overall solar-to-electrical energy conversion efficiency of the photovoltaic cells was improved by the contribution of photosensitizing effect in the wavelength range derived from the electron-acceptor components rather than the squarylium component. This phenomenon implies the possibility that the electron-accepting group acts as an anchoring unit to the TiO_2 surface.

1. Introduction

Dye-sensitized solar cells (DSSCs) have attracted significant attention as high-efficiency and cost-effective photovoltaic cells for the conversion of solar energy, along with bulk heterojunction solar cells consisting of conjugated polymer-fullerene blends [1–3]. The utilization of nanocrystalline TiO_2, which affords a vast surface area, and the development of Ru(II)–polypyridyl-complexes such as N3 [4], N719 [5], and black dye [6] has made it possible to obtain high solar energy-to-electricity conversion efficiency (η) of up to 11% under solar simulation (AM 1.5 G) irradiation [7]. As an alternative to Ru complexes, metal-free organic dyes have also been utilized as sensitizers of DSSCs because they have advantages such as a high molar absorption coefficient, facile modification of dye structures, tunable absorption properties through molecular design, and cost-effectiveness [8]. Efforts are underway to improve the molecular design of metal-free sensitizing dyes to obtain a higher conversion efficiency comparable to that of Ru complex-based DSSCs. Recently, numerous organic sensitizers, such as coumarin [9,10], indoline [11–14], cyanine [15–17], and others [18–22], have been identified, and photovoltaic performances of DSSCs based on these dyes have been gradually improved, resulting in a maximum conversion efficiency of 9.5% [12]. These results indicate that increasing the flexibility of the dye design expands the potential for modifying the cell performance.

Squarylium dyes are well known for their unique optical properties, such as intense and sharp light absorption in the visible to NIR region [23]. The optical band gap of these dyes can be tuned through the choice of electron-rich aromatic/heterocyclic components and the linear extension of the cyclobutene core. In addition, the electron distribution of the HOMO and LUMO of squarylium dyes are influenced by the molecular symmetry and functionality on the aromatic/heterocyclic components. Various types of symmetrical and nonsymmetrical squarylium dyes have been prepared and used in a wide range of applications, such as chemosensors [24–29], noncovalent fluorescent probes for bioanalysis [30–33], organic light-emitting diodes [34–36], supramolecular architectures [37,38] and bulk heterojunction solar cells [39,40]. One of the applications that has attracted the most attention is the use of squarylium dyes as metal-free sensitizers for DSSCs [41–46]. Various types of squaryliums have been used as sensitizers for wide

* Corresponding authors. Tel.: +81 72 254 9329; fax: +81 72 254 9910.
E-mail addresses: tmaeda@chem.osakafu-u.ac.jp (T. Maeda), nakazumi@chem.osakafu-u.ac.jp (H. Nakazumi).

0143-7208/$ – see front matter © 2011 Elsevier Ltd. All rights reserved.
doi:10.1016/j.dyepig.2011.01.006

band gap semiconductors, and some features associated with molecular design have been elucidated. Nazeerudin et al. achieved high conversion efficiency ($\eta = 4.5\%$) by the use of an unsymmetrical indole-based squarylium dye bearing carboxylic groups directly attached to the indole components [47]. The squarylium was designed in such a way that electrons unidirectionally flowed from the light-harvesting components of the sensitizer to the semiconductor surface. For further improvement of the performance of cells based on squaryliums, the appropriate design of dye molecules, in order to enable efficient electron injection into the conduction band, will be needed along with control of the adsorption properties of dyes.

In this paper, we report the synthesis of novel squarylium dyes bearing terminally connected strong electron-acceptor components and their application as sensitizers for TiO_2-based DSSCs (Fig. 1). Tetracyanoquinodimethane (TCQ), tetracyanoanthraquinodimethane (TCAQ), and TCAQ with a hydroxyl group as an anchoring group (TCAQH) were chosen as electron-accepting units, and were incorporated in a *N*,*N*-dialkylanilino-squaraine and a squaraine consisting of indolenine and *N*,*N*-dialkylaniline components through ester linkages. Then, the effect of the incorporation of strong electron acceptors on the photovoltaic performance is discussed together with the effect of various dying conditions.

2. Experimental

2.1. General

The NMR spectra were obtained using a JEOL JNM LA-400 spectrometer operating at 400 MHz for ^{1}H NMR and 100 MHz for ^{13}C NMR. Chemical shifts are reported in parts per million (δ) downfield from tetramethylsilane (TMS) as an internal standard in $CDCl_3$. MALDI-TOF MS spectra were recorded on a Shimazu AXIMA spectrometer. The elemental analyses were performed on a Yanako CHN CORDER JM-10 analyzer. The IR spectra were recorded using a Shimazu FT-IR 8400S spectrophotometer. The absorption spectra and fluorescence emission spectra were measured in a 1.0 cm quartz cell on a Shimazu UV-3100 spectrophotometer and a Shimazu RF-5000 spectrofluorometer. The oxidation potential of the dye was measured with a Hokuto Denko HZ-5000 electrochemical measurement system at a scanning rate of 100 mV s^{-1}, equipped with a normal one-compartment cell with a Pt working electrode, a Pt counter electrode, and a Ag/Ag^+ reference electrode. The measurement was performed in an acetonitrile solution including 0.1 M tetrabutylammonium perchlorate as a supporting electrolyte. 3-[4-(Dibutylamono) phenyl]-4-hydroxycyclobut-3-ene-1,2-dione was prepared from *N*,*N*-dibutylaniline and squaryl chloride obtained by a reaction of squaric acid with thionyl chloride according to the conventional method [48]. 2-(*N*-methylphenylamino)ethanol (**3**), 1-(2-hydroxyethyl)-2,3,3-trimethyl-3*H*-indolium iodide (**8**), were prepared according to the conventional synthesis [48,49]. 7,7,8,8-Tetracyano-*p*-quinodimethanepropionic acid (**4**) [50], 3-[2′-(11,11,12,12-tetracyano-9,10-anthraquinodimethane)methoxicarbonyl]propionic acid (**5**) [51], and 2,6-dihydroxy-11,11,12,12-tetracyanoanthraquinodimethane (**7**) [52] were synthesized by the previously reported methods. Dicyclohexylcarbodiimide (DCC), 1-ethyl-3-(3-dimethylaminopropyl)carbodiimide hydrochloride (EDC-HCl), 4-(dimethylamino)pyridine (DMAP), succinic anhydride, pyridine, and quinoline were purchased from Tokyo Chemical Industry and Wako Pure Chemical and used as received. Organic solvents for the preparation of the compounds were purchased as anhydrous reagent grade and used as received.

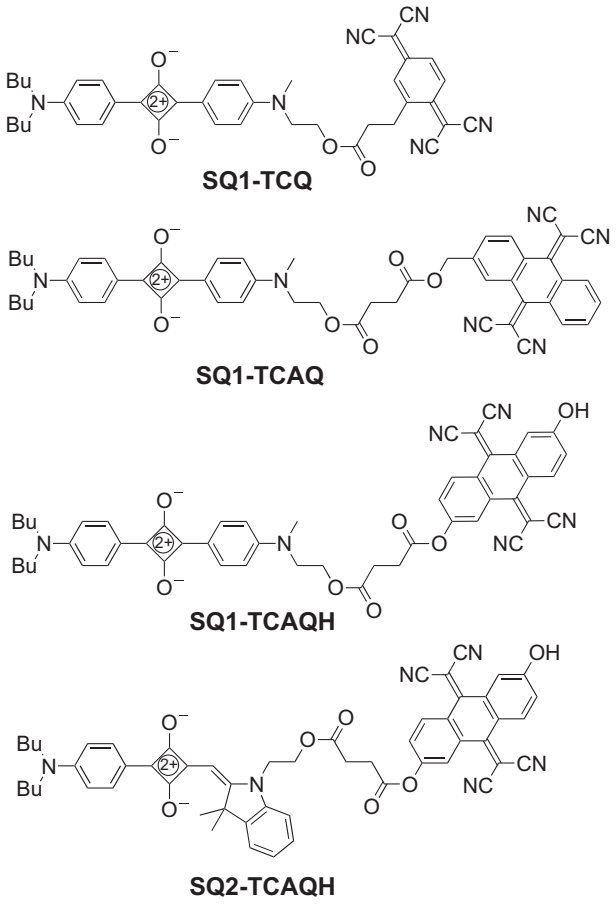

Fig. 1. Molecular structures of the squarylium-based diads.

2.2. Preparation of ***SQ1-TCQ***

2.2.1. Compound ***2***

3-[4-(Dibutylamono)phenyl]-4-hydroxycyclobut-3-ene-1,2-dione (**1**) (6.0 g, 20 mmol) and 2-(*N*-methylphenylamino)ethanol (**3**) (3.0 g, 20 mmol) were dissolved in a mixture of 2-propanol and triethoxymethane (20 mL, 5/1, v/v) under Ar atmosphere and the solution was heated under reflux for 13 h. After cooling, the solvent was removed on a rotary evaporator, and the residue was purified by silica gel column chromatography (eluent; CH_2Cl_2/MeOH, 20/1, v/v), followed by washing with CH_2Cl_2 to afford squarylium **2** as a green solid (4.3 g, 49%). Mp 188–190 °C (lit. [53] mp 188–190 °C). ^{1}H NMR ($CDCl_3$): δ 0.99 (t, $J = 7.2$ Hz, 6H, $-CH_3$), 1.40 (m, 4H, $-CH_2-$), 1.63–1.65 (m, 4H, $-CH_2-$), 3.17 (s, 3H, NCH_3), 3.26 (br s, 1H, OH), 3.44 (t, $J = 7.8$ Hz, 4H, NCH_2-), 3.68 (t, $J = 5.6$ Hz, 2H, NCH_2-), 3.92 (m, 2H, $-CH_2O$), 6.73 (d, $J = 9.6$ Hz, 2H, ArH), 6.77 (d, $J = 9.6$ Hz, 2H, ArH), 8.26 (d, $J = 9.3$ Hz, 2H, ArH), 8.34 (d, $J = 9.3$ Hz, 2H, ArH). ^{13}C NMR ($CDCl_3$): δ 13.84, 20.21, 29.57, 39.61, 51.22, 55.01, 59.91, 112.39, 112.56, 119.26, 119.76, 133.05, 133.16, 153.48, 154.74, 183.53, 186.59. IR (KBr): 3418, 2949, 2922, 1589, 1414, 1194 cm^{-1}. MALDI-TOF MS: *m/z* 434.19 ($[M]^+$).

2.2.2. Compound ***SQ1-TCQ***

7,7,8,8-Tetracyano-*p*-quinodimethanepropanoic acid (**4**) (0.14 g, 0.50 mmol), squarylium **2** (0.22 g, 0.5 mmol), DCC (0.10 g, 0.5 mmol), and DMAP (61 mg, 0.50 mmol) were dissolved in CH_2Cl_2 (25 mL) and the mixture was stirred for 2 h at room temperature. The reaction mixture was directly purified by silica gel column chromatography (eluent; CH_2Cl_2/MeOH, 95/5, v/v), followed by recrystallization, where the crystal was grown by slow diffusion from $CHCl_3$ solution to acetonitrile. The resulting material was further purified by recrystallization from $CHCl_3$ to afford **SQ1-TCQ**

as brown crystals (48 mg, 13%). Mp 217 °C (decomp). ^{1}H NMR ($CDCl_3$): δ 1.00 (t, J = 9.0 Hz, 6H, $-CH_3$), 1.38–1.42 (m, 4H, $-CH_2-$), 1.63–1.67 (m, 4H, $-CH_2-$), 2.58 (t, J = 6.0 Hz, 2H, $-CH_2-$), 3.16 (s, 3H, NCH_3), 3.17 (t, J = 6.0 Hz, 2H, $-CH_2-$), 3.46 (t, J = 6.0 Hz, 4H, NCH_2-), 3.81 (t, J = 6.0 Hz, 2H, NCH_2-), 4.41 (t, J = 6.0 Hz, 2H, OCH_2-), 6.75 (d, J = 9.0, Hz, 2H, ArH), 6.80 (d, J = 9.0 Hz, 2H, ArH), 7.19 (s, 1H, ArH), 7.32 (d, J = 9.0 Hz, 1H, ArH), 7.51 (d, J = 9.0 Hz, 1H, ArH), 8.28 (d, J = 9.0 Hz, 2H, ArH), 8.38 (d, J = 9.0 Hz, 2H, ArH). IR (KBr): 2216, 2180, 1726, 1610, 1585 cm^{-1}. MALDI-TOF MS: m/z 693.14 ([M + H]$^+$). Anal. Calcd for $C_{42}H_{40}N_6O_4 \cdot 0.5H_2O$: C, 71.88; H, 5.89; N, 11.97. Found: C, 71.65; H, 5.84; N, 11.90%.

2.3. Preparation of *SQ1-TCAQ*

3-[2′-(11,11,12,12-Tetracyano-9,10-anthraquinodimethane)methoxicarbonyl]propionic acid (**5**) (87 mg, 0.20 mmol), EDC-HCl (38 mg, 0.20 mmol), and DMAP (24 mg, 0.20 mmol) were dissolved in CH_2Cl_2 (4 mL). The mixture was stirred for 30 min at room temperature, then squarylium **2** (87 mg, 0.20 mmol) was added and stirred for 1 h at room temperature. The reaction mixture was directly purified by silica gel column chromatography (eluent; CH_2Cl_2/MeOH, 94/6, v/v), followed by recrystallization, where the crystal was grown by slow diffusion from $CHCl_3$ solution to acetonitrile to afford **SQ1-TCAQ** as dark green crystals (110 mg, 65%). Mp 217–220 °C ^{1}H NMR (DMSO-d_6): δ 0.92 (t, J = 6.0 Hz, 6H, $-CH_3$), 1.29–1.37 (m, 4H, $-CH_2-$), 1.50–1.59 (m, 4H, $-CH_2-$), 2.53 (t, J = 6.0 Hz, 2H, $-CH_2-$), 2.61 (t, J = 6.0 Hz, 2H, $-CH_2-$), 3.11 (s, 3H, NCH_3), 3.50 (t, J = 9.0 Hz, 4H, NCH_2-), 3.80 (t, J = 6.0 Hz, 2H, NCH_2), 4.25 (t, J = 6.0 Hz, 2H, OCH_2), 5.24 (s, 2H, OCH_2), 6.92 (d, J = 6.0 Hz, 2H, ArH), 6.95 (d, J = 6.0 Hz, 2H, ArH), 7.76 (d, J = 9.0 Hz, 1H, ArH), 7.83 (d, J = 6.0 Hz, 1H, ArH), 7.84 (d, J = 6.0 Hz, 1H, ArH), 8.05–8.09 (m, 4H, ArH), 8.15–8.18 (m, 2H, ArH), 8.21–8.25 (m, 2H, ArH). ^{13}C NMR (DMSO-d_6): δ 13.72, 19.48, 28.41, 28.55, 28.83, 29.21, 38.75, 49.87, 50.20, 50.43, 61.52, 64.26, 82.94, 83.26, 110.67, 112.96, 113.20, 113.90, 113.98, 118.35, 119.10, 125.52, 127.32, 127.40, 127.45, 129.40, 130.01, 130.05, 130.33, 130.60, 131.13, 132.08, 132.16, 140.92, 153.74, 153.90, 159.58, 159.61, 171.54, 171.75, 181.62, 184.84, 186.93. IR (KBr): 3458, 2957, 2927, 2221, 1733, 1610, 1586, 1394, 1356, 1175, 783 cm^{-1}. MALDI-TOF MS: m/z 850.28 ([M]$^+$). Anal. Calcd for $C_{52}H_{46}N_6O_6 \cdot 0.5H_2O$: C, 72.63; H, 5.51; N, 9.77. Found: C, 72.67; H, 5.57; N, 9.68%.

2.4. Preparation of *SQ1-TCAQH*

2.4.1. Compound *6*

To the solution of squarylium **2** (0.44 g, 1.0 mmol) in CH_2Cl_2 (50 mL) was added succinic anhydride (0.80 g, 8.0 mmol), DMAP (1.0 g, 8.0 mmol), and pyridine (0.80 g, 10 mmol). The reaction mixture was stirred at room temperature for 3 h, and quenched with ice water and extracted with $CHCl_3$. The organic layer was washed with H_2O, dried over $MgSO_4$, and evaporated under reduced pressure. The crude product was purified by silica gel column chromatography (eluent; CH_2Cl_2/MeOH, 95/5, v/v), followed by recrystallization from $CHCl_3$–acetonitrile to afford **6** as dark green crystals (0.18 g, 33%). Mp 211–213 °C ^{1}H NMR (DMSO-d_6): δ 0.93 (t, J = 6.0 Hz, 6H, $-CH_3$), 1.32–1.40 (m, 4H, $-CH_2-$), 1.53–1.61 (m, 4H, $-CH_2-$), 2.40–2.48 (m, 4H, $-CH_2-$), 3.16 (s, 3H, NCH_3), 3.52 (t, J = 6.0 Hz, 4H, NCH_2-), 3.83 (t, J = 6.0 Hz, 2H, NCH_2-), 4.27 (t, J = 6.0 Hz, 2H, OCH_2-), 6.96–6.99 (m, 4H, ArH), 8.12 (d, J = 9.0 Hz, 2H, ArH), 8.14 (d, J = 9.0 Hz, 2H, ArH), 12.2 (br s, 1H, OH). ^{13}C NMR (DMSO-d_6): δ 13.72, 19.48, 28.51, 28.67, 29.21, 38.91, 50.31, 50.42, 61.41, 112.98, 113.24, 118.38, 119.11, 131.15, 132.10, 153.76, 153.87, 172.03, 173.28, 181.63, 184.93, 187.02. IR (KBr): 3451, 2956, 2927, 1733, 1593, 1388, 1360, 1187, 786 cm^{-1}. MALDI-TOF MS: m/z 534.30 ([M]$^+$). Anal. Calcd for $C_{31}H_{38}N_2O_6 \cdot 0.5H_2O$: C, 68.49; H, 7.23; N, 5.15. Found: C, 68.81; H, 6.96; N, 5.05%.

2.4.2. Compound *SQ1-TCAQH*

Compound **3** (53 mg, 0.10 mmol), EDC-HCl (19 mg, 0.10 mmol), and DMAP (12 mg, 0.10 mmol) were dissolved in THF (4 mL). The mixture was stirred for 20 min, and then added 2,6-dihydroxy-11,11,12,12-tetracyanoanthraquinodimethane (**7**) (34 mg, 0.10 mol). After stirring for 15 h at room temperature, the solvent was removed on a rotary evaporator, and the residue was purified by silica gel column chromatography (eluent; CH_2Cl_2/MeOH, 98/2, v/v), followed by recrystalization from acetonitrile to afford **SQ1-TCAQH** as blue crystals (46 mg, 53%). Mp 235 °C (decomp). ^{1}H NMR (DMSO-d_6): δ 0.93 (t, J = 6.0 Hz, 6H, $-CH_3$), 1.30–1.41 (m, 4H, $-CH_2-$), 1.52–1.63 (m, 4H, $-CH_2-$), 2.65 (t, J = 6.0 Hz, 2H, $-CH_2-$), 2.87 (t, J = 6.0 Hz, 2H, $-CH_2-$), 3.15 (s, 3H, NCH_3), 3.52 (t, J = 6.0 Hz, 4H, NCH_2), 3.86 (t, J = 6.0 Hz, 2H, NCH_2), 4.28–4.35 (m, 2H, OCH_2-), 6.96 (d, J = 6.0 Hz, 2H, ArH), 6.99 (d, J = 6.0 Hz, 2H, ArH), 7.18–7.23 (m, 1H, ArH), 7.56 (dd, J = 3.0, 9.0 Hz, 1H, ArH), 7.59–7.65 (m, 1H, ArH), 7.92 (d, J = 3.0 Hz, 1H), 8.10 (d, J = 9.0 Hz, 1H, ArH), 8.08–8.12 (m, 1H, ArH), 8.13 (d, J = 6.0 Hz, 2H, ArH), 8.24 (d, J = 6.0 Hz, 2H, ArH), 11.3 (br s, 1H, −OH). ^{13}C NMR (DMSO-d_6): 13.73, 19.49, 28.60, 28.73, 29.22, 50.25, 50.44, 61.68, 80.53, 83.03, 113.00, 113.25, 113.85, 114.09, 114.22, 114.42, 118.37, 118.84, 119.11, 120.36, 120.46, 125.09, 127.67, 129.17, 129.96, 131.12, 132.13, 132.34, 132.38, 152.27, 153.79, 153.90, 158.85, 159.26, 160.98, 170.38, 171.63, 181.62, 184.84, 187.06. IR (KBr): 3435, 2958, 2928, 2224, 1587, 1384, 1361, 1179, 785 cm^{-1}. MALDI-TOF MS: m/z 852.50 ([M]$^+$). Anal. Calcd for $C_{51}H_{44}N_6O_7 \cdot H_2O$: C, 70.33; H, 5.32; N, 9.65. Found: C, 70.53; H, 5.19; N, 9.42%.

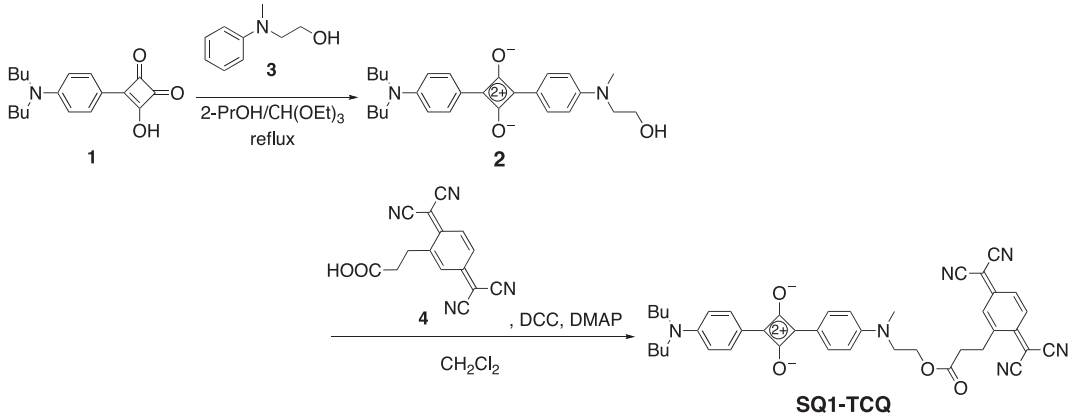

Scheme 1.

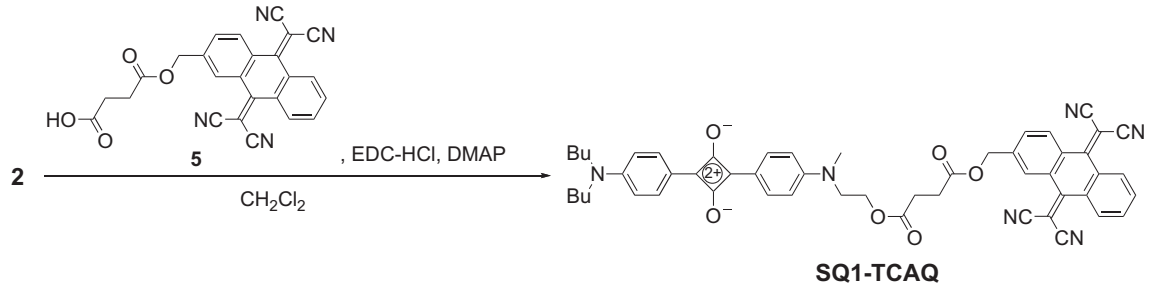

Scheme 2.

2.5. Preparation of ***SQ2-TCAQH***

2.5.1. Compound ***9***

Compound **1** (0.25 g, 0.83 mmol) and 1-(2-hydroxyethyl)-2,3,3-trimethyl-3*H*-indolium bromide (**8**) (0.23 g, 0.82 mmol) were dissolved in a mixture of 1-butanol (24 mL) and benzene (6 mL) under Ar atmosphere. Then a few drops of quinoline were added and the solution was heated at 100 °C for 4 h. After cooling, the solvent was removed on a rotary evaporator, and the residue was purified by silica gel column chromatography (eluent; $CHCl_3$/MeOH, 10/1, v/v), and dried to afford **9** as a green crystal (0.10 g, 25%). Mp 225 °C ^{1}H NMR ($CDCl_3$): δ 0.98 (t, J = 6.0 Hz, 6H, $-CH_3$), 1.33–1.42 (m, 4H, $-CH_2-$), 1.56–1.65 (m, 4H, $-CH_2-$), 1.70 (s, 6H, $-CH_3$), 3.38 (t, J = 6.0 Hz, 4H, NCH_2), 4.09 (t, J = 6.0 Hz, 2H, NCH_2-), 4.48 (t, J = 6.0 Hz, 2H, OCH_2-), 4.72 (s, 1H, OH), 6.12 (s, 1H, =CH–), 6.67 (d, J = 9.0 Hz, 2H, ArH), 7.21–7.26 (m, 2H, ArH), 7.34–7.39 (m, 2H, ArH), 8.22 (d, J = 9.0 Hz, 2H). IR (KBr): 3327, 2930, 1628, 1576, 1418, 1312, 1184 cm^{-1}. MALDI-TOF MS: *m/z* 487.79 ($[M + H]^+$ = 487.29). Anal. Calcd for $C_{31}H_{38}N_2O_3 \cdot 0.2H_2O$: C, 75.95; H, 7.89; N, 5.71. Found: C, 75.88; H, 8.03; N, 5.71%.

2.5.2. Compound ***10***

This compound was synthesized by a similar procedure to the preparation of **6**. The crude product was purified by silica gel column chromatography (eluent; CH_2Cl_2/MeOH, 95/5, v/v), and the resulting product was used in next step without further purification.

10: Yield 65%. ^{1}H NMR (DMSO-d_6): δ 0.93 (t, J = 6.0 Hz, 6H, $-CH_3$), 1.35 (m, 4H, $-CH_2-$), 1.55 (m, 4H, $-CH_2-$), 1.72 (s, 6H, CH_3), 2.29 (m, 4H, $-CH_2-$), 3.40 (m, 4H, NCH_2-), 4.50 (m, 2H, NCH_2-), 4.60 (m, 2H, OCH_2-), 6.13 (s, 1H, =CH–), 6.81 (d, J = 9.0 Hz, 2H, ArH), 7.29–7.35 (m, 1H, ArH), 7.41–7.48 (m, 1H, ArH), 7.52–7.60 (m, 1H, ArH), 7.60–7.66 (m, 1H, ArH), 8.03 (d, J = 9.0 Hz, 2H, ArH), 12.08 (s, 1H, –OH).

2.5.3. SQ2-TCAQH

This compound was obtained by a similar procedure for the preparation of **SQ1-TCAQH**.

SQ2-TCAQH: Yield 13%. Mp 230 °C (decomp). ^{1}H NMR (DMSO-d_6): δ 0.98 (t, J = 6.0 Hz, 6H, $-CH_3$), 1.31–1.44 (m, 4H, $-CH_2-$), 1.52–1.65 (m, 4H, $-CH_2-$), 1.84 (s, 6H, $-CH_3$), 2.57–2.70 (m, 2H, $-CH_2-$), 2.75–2.90 (m, 2H, $-CH_2-$), 3.41 (t, J = 6.0 Hz, 4H, NCH_2), 4.40–4.68 (m, 4H, $-NCH_2CH_2O-$), 6.28 (s, 1H, =CH–), 6.74 (d, J = 9.0 Hz, 2H, ArH), 7.06 (dd, J = 9.0, 3.0 Hz, 1H, ArH), 7.17–7.22 (m, 1H, ArH), 7.28–7.33 (m, 1H, ArH), 7.35–7.45 (m, 3H, ArH), 7.68 (s, 1H, ArH), 7.85 (d, J = 9.0 Hz, 1H, ArH), 8.05–8.08 (m, 2H, ArH), 8.27 (d, J = 9.0 Hz, 2H, ArH), 12.92 (br s, 1H, OH).IR (KBr): 2953, 2926, 2226, 1605, 1558, 1522, 1420, 1312, 1178, cm^{-1}. MALDI-TOF MS: *m/z* 904.36 ($[M]^+$). HRMS (FAB): calcd for $C_{55}H_{49}N_6O_7$ (**SQ1-TCAQH** + H^+) *m/z* 905.3663; found *m/z* 905.3668.

2.6. General procedure for fabrication of the nanocrystalline TiO_2 solar cells

Transparent TiO_2 photoelectrodes (~12 μm thick, 5 mm × 5 mm) were fabricated by screen-printing. Nanocrystalline TiO_2 paste [PST-18NR (particle size; *ca.* 20 nm), JGC Catalysts and Chemicals Ltd, Japan] was printed twice on the F-doped SnO_2 substrate (Nippon Sheet Glass, 4 mm thick). After drying 125 °C for 10 min, TiO_2 paste consisting of large TiO_2 particle (*ca.* 400 nm, JGC Catalysts and Chemicals Ltd, Japan) was coated on it as a scattering center. The resulting substrate was gradually heated and sintered at 500 °C for 15 min. After cooling, the sintered TiO_2 films with an area of 0.25 cm^2 were impregnated in a 40 mM $TiCl_4$ aqueous solution at

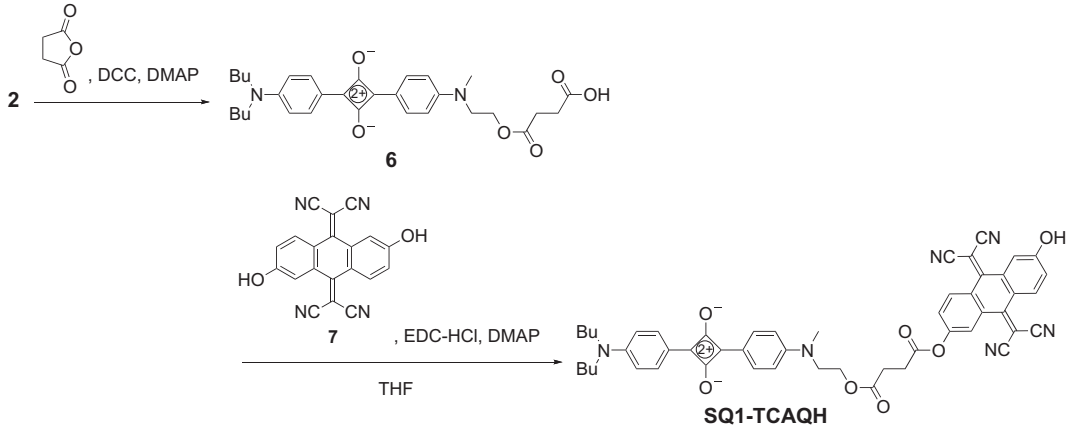

Scheme 3.

70 °C for 30 min and then washed with distilled water and methanol. After drying under reduced pressure, treated TiO_2 films were sintered again at 500 °C for 30 min. The resulting TiO_2 photoelectrodes were immersed in a solution of dyes (0.12 mM) and chenodeoxycholic acid (CDCA, 6 mM) in *t*-BuOH/acetonitrile and then kept at ambient temperature overnight, followed by washing with acetonitrile to remove non-adsorbed dye. In case of CDCA-free condition, TiO_2 photoelectrodes were dyed at 80 °C for 1 h. The dye-adsorbed TiO_2 film and a Pt-coated ITO grass substrate were separated by Teflon spacer (25 μm thick), which had tiny two cuts for injection of the electrolyte and then clipped. The electrolyte consisting of 0.24 M 1,2-dimethyl-3-*n*-propylimidazolium iodide (DMPImI), 0.07 M LiI, and 0.018 M I_2 in $CHCl_3$/acetonitrile (1/1, v/v) was introduced into the interspace between the TiO_2 photoelectrode and the Pt counter electrode to obtain the sandwich cell.

2.7. Photovoltaic measurements of the solar cells

The photovoltaic performance of the DSSC was measured by using AM 1.5 solar simulator (CEP-2000, Bunko-Keiki, Japan) equipped with a source meter (Keithley 2400). The incident light intensity was calibrated with a standard Si solar cell. To prevent an over estimation of the energy conversion efficiency, a black mask was used. The incident photon-to-current conversion efficiency (IPCE) was measured using an action spectrum measurement system connected to a solar simulator (CEP-2000, Bunko-Keiki, Japan).

3. Results and discussion

3.1. Synthesis of squarylium-based diads

The *N*,*N*-dialkylanilino-squaraine bearing a hydroxyl group (**2**) was prepared by condensation of aniline derivative (**3**) with a monocondensation product of squaric acid and *N*,*N*-dibutylaniline (**1**) (Scheme 1). Then, squarylium **2** was reacted with a TCQ derivative bearing a carboxylic acid (**4**) to obtain the squarylium-TCQ diad (**SQ1-TCQ**). The squarylium-TCAQ diad (**SQ1-TCAQ**) was also prepared from squarylium **2** and a TCAQ derivative with a carboxyl group (**5**) (Scheme 2). The squarylium-TCAQ diad having a hydroxyl group (**SQ1-TCAQH**) was prepared by the condensation of a precursor dye **6** prepared from **2** and succinic anhydride with 2,6-dihydroxy-11,11,12,12-tetracyanoanthraquinodimethane (**7**) (Scheme 3). In order to examine the effect of the dye structure on photosensitization of TiO_2, a squarylium dye consisting of *N*,*N*-dibutylaniline and 1-(2-hydroxyethyl)-2,3,3-trimethylindolium was used as a dye component for the squarylium-TCAQ diad (Scheme 4). The condensation reaction of the semisquarylium (**1**) with the corresponding indolium salt under azeotropic conditions in the presence of quinoline afforded the desired squarylium dye with a hydroxyl group (**9**). Squarylim **9** was converted to the carboxy precursor **10**. Then, the nonsymmetrical squarylium-TCAQ diad with a phenolic hydroxyl group (**SQ2-TCAQH**) was successfully synthesized by the condensation of **10** with TCAQ derivative **7**.

3.2. Light-absorbance, fluorescent emission, and electrochemical properties of squarylium-based diads

The absorption spectra of the obtained dyes in $CHCl_3$ (5.0 μM) at 298 K are displayed in Fig. 2a, and the detailed absorption properties are summarized in Table 1. Diads consisting of anilino-squarylium (**SQ1-TCQ**, **SQ1-TCAQ**, and **SQ1-TCAQH**) exhibited almost the same absorption properties, except for the absorption band for electron-accepting components. These dyes have absorption maxima at 632–633 nm with a molar absorption coefficient (ε_{abs}) of 3.3–3.5 × 10^5 M^{-1} cm^{-1}. **SQ2-TCAQH** exhibited the absorption maximum at a slightly longer wavelength and its molar absorption coefficient (ε_{abs}) was 2.7 × 10^5 M^{-1} cm^{-1}. In addition to sharp absorption of the corresponding squarylium component, absorptions corresponding to the TCQ and TCAQ moieties were also observed. Squarylium dyes having the TCAQ moiety showed a broad absorption at less than 500 nm. Thus, all dyes exhibited an intense and sharp absorption in the far-red region. The fluorescence emission spectra of the obtained dyes are shown in Fig. 2b. These dyes exhibited fluorescence emissions at almost the same wavelength with a small Stokes' shifts. To get an efficient charge separation, the LUMO of the dye should be more negative than the conduction band edge of TiO_2 (E_{cb}), and the HOMO of the dye should be more positive than the redox potential of I^-/I_3^-. Based on the cyclic voltammetry measurement, the first oxidation potential (E_{ox}) corresponding to the HOMO level of **SQ2-TCAQH** (0.69 V *vs.* NHE) was sufficiently more positive than the I^-/I_3^- redox potential. In addition, the LUMO level estimated by the HOMO level and the 0–0 transition energy calculated from the wavelength where the normalized absorption and fluorescence

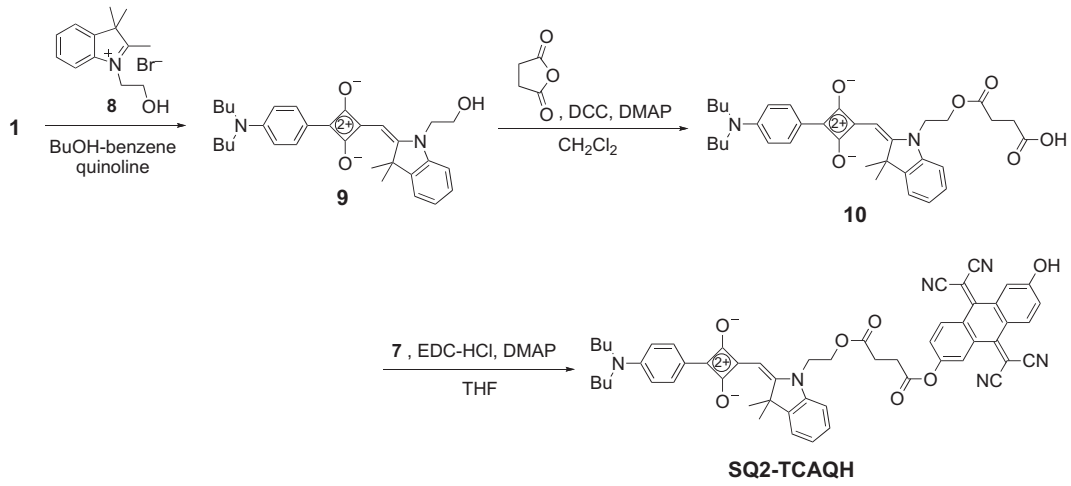

Scheme 4.

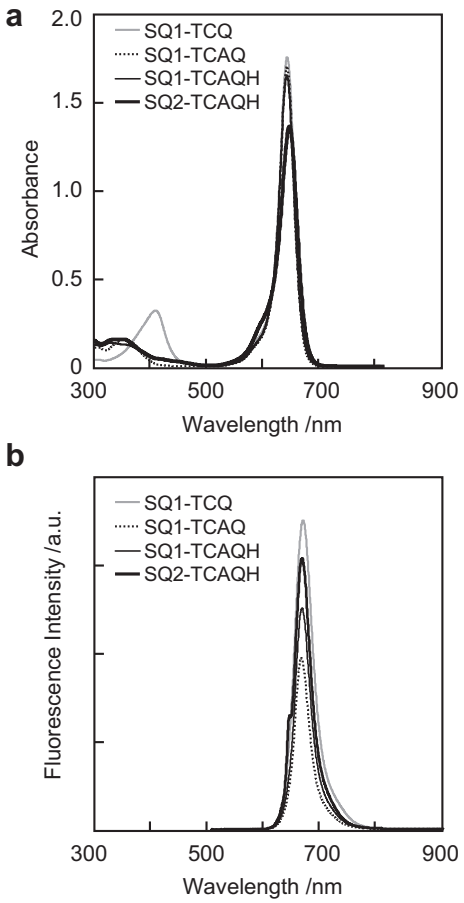

Fig. 2. Electronic absorption (a) and fluorescence emission spectra (b) of **SQ1-TCQ** (gray), **SQ1-TCAQ** (dotted), **SQ1-TCAQH** (plain), and **SQ2-TCAQH** (bold) in $CHCl_3$ at 298 K. Dye concentrations were adjusted to 5.0 μM.

Table 1
Electronic absorption data of squarylium derivatives (5×10^6 M in $CHCl_3$, 298 K).

Dye	λ_{abs}/nm	λ_{em}/nm	ε_{abs}/M^{-1} cm^{-1}
SQ1-TCQ	633	656	350000
SQ1-TCAQ	632	656	340000
SQ1-TCAQH	633	655	329000
SQ2-TCAQH	637	665	271000

spectra intersect (−1.18 V *vs.* NHE) was also sufficiently more negative than the E_{cb} (−0.5 V *vs.* NHE) [54].

3.3. Photovoltaic performance of DSSCs sensitized with squarylium-based diads

To investigate the photovoltaic properties, DSSCs sensitized with squarylium-based diads were prepared using nanocrystalline TiO_2 photoelectrodes. The open-circuit photovoltage (V_{oc}), short-circuit photocurrent density (J_{sc}), fill factor (ff), and solar-to-electrical energy conversion efficiencies (η) of DSSCs are summarized in Table 2. The photon-to-current conversion efficiencies (IPCE) and the current density−voltage (J–V) curves are shown in Fig. 3a and b, respectively. Action spectra of IPCEs for **SQ1-TCQ** and **SQ1-TCAQ** exhibited quite low values, indicating that squarylium dyes without hydroxyl groups were ineffective for sensitization of TiO_2. In contrast, **SQ1-TCAQH** and **SQ2-TCAQH**, which have hydroxyl groups

Table 2
Photovoltaic performance of DSSCs conducted using squarylium-based dyes[a]

Dye	J_{sc}/mA cm^{-2}	V_{oc}/V	Fill factor	η/%
SQ1-TCQ	0.81	0.53	0.65	0.28
SQ1-TCAQ	0.39	0.46	0.64	0.11
SQ1-TCAQH	1.26	0.55	0.66	0.46
SQ2-TCAQH	2.36	0.66	0.71	1.10

[a] Conditions: irradiated light, AM 1.5 (100 mW cm^{-2}); dying condition, 120 μM dyes and 6 mM CDCA in acetonitrile/*t*-BuOH at room temperature.

on TCAQ components, gave higher IPCE values in the range from 500 to 700 nm than the dyes without hydroxyl groups. Therefore, the hydroxyl groups of **SQ1-TCAQH** and **SQ2-TCAQH** play an important role as the anchoring groups for the TiO_2 surface. The similarity between the IPCE spectra and the absorption spectra of **SQ1-TCAQH** and **SQ2-TCAQH** indicated that the photocurrent was attributable to the photosensitizing effect of squarylium-based diads. The photovoltaic performance for DSSCs based on the nonsymmetrical squarylium-based diad **SQ2-TCAQH** was superior to that of the symmetrical squarylium-based diad **SQ1-TCAQH**. Das et al. pointed out the importance of the nonsymmetrical structure of squaryliums for the efficient electron injection originating from unidirectional electron flow from dyes to the TiO_2 conduction band [42]. In the nonsymmetrical squarylium dyes consisting of *N*,*N*-dialkylaniline and heterocyclic components linked through the methylene spacer, it is noted that the HOMO-LUMO excitation moved the electron distribution from the *N*,*N*-dialkylaniline moiety

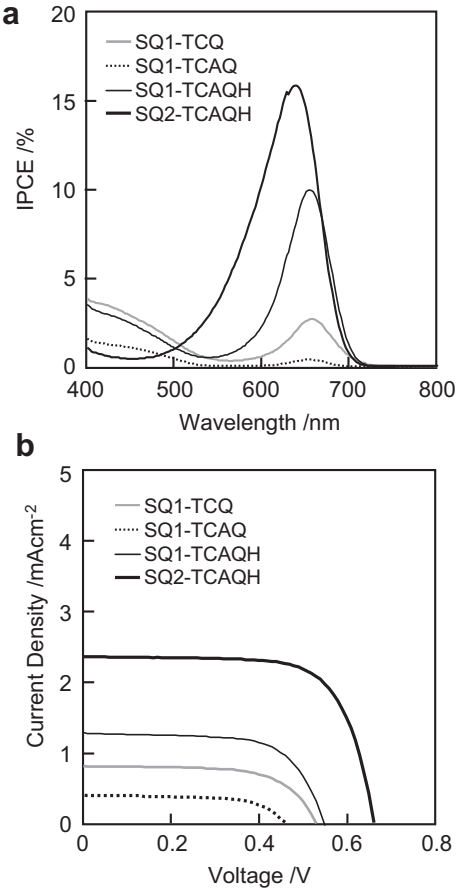

Fig. 3. Spectra of incident photon-to-current conversion efficiency (IPCE) (a) and J–V curves (b) of DSSCs prepared with **SQ1-TCQ** (gray), **SQ1-TCAQ** (dotted), **SQ1-TCAQH** (plain), and **SQ2-TCAQH** (bold).

to the heterocycle with the methylene spacer. In the case of **SQ2-TCAQH**, these effects based on the nonsymmetrical structure of squaryliums should contribute to the photovoltaic performance. Although the η value and J_{sc} value of the DSSC based on **SQ2-TCAQ** were still low, a V_{oc} value of 0.66 V was achieved, which was the highest V_{oc} value obtained so far among squarylium dye-based DSSCs. This might imply that the diad structure comprised of the strong electron-accepting component and the light-harvesting squarylium component contributed to the unidirectional flow of electrons from the light-harvesting components of the sensitizer to the semiconductor surface and thereby minimized the charge recombination of injected electrons with dye cations and I_3^-.

3.4. Dying conditions for DSSCs sensitized with squarylium-based diads

In general, acids such carboxylic acid or phosphoric acid are used as the anchoring units for adsorption of dyes onto the TiO_2 surface. In the case of squarylium-based diads, the hydroxyl group on the TCAQ component should work as an anchoring unit for adsorption of the squarylium-based diad **SQ2-TCAQH** onto the TiO_2 surface. DSSCs based on **SQ2-TCAQH** were prepared by dying with CDCA as a coadsorbent to prevent dye aggregation on the surface. However, this method would be ineffective for adequate absorption of the dye due to low loading of the dye and preferential adsorption of CDCA stemming from the lower acidity of the hydroxyl group relative to that of the carboxylic acid of CDCA. To improve the dye adsorption on the TiO_2 surface, DSSCs were prepared by dying at 80 °C without CDCA and their photovoltaic performances were evaluated (Table 3). First, we examined the influence of the concentration of **SQ2-TCAQH** on the efficiency of the DSSC. The η value increased with decreasing concentration of the dye and reached a peak at 15 μM. Fig. 4 shows the absorption spectra of **SQ2-TCAQH** in $CHCl_3$ and on TiO_2 films prepared from 15 to 30 μM solutions of **SQ2-TCAQH**. The absorption spectra of **SQ2-TCAQH** on TiO_2 were broadened compared to those of the solution state, indicating strong interactions between the dyes and the TiO_2 surface. In a TiO_2 film dying at 30 μM, a seriously broadened and blue-shifted strong absorption was clearly observed. This absorption would be attributable to H-type aggregation of dyes on the TiO_2 surface, which would allow the quenching process between the aggregated dyes [55]. Thus, the decrease of the η value of DSSCs dyed at concentrations of 30 μM or higher was due to the aggregation effect. Interestingly, the broad peak around 475 nm was newly observed in the action spectra of IPCE as a result of the change in dying conditions (Fig. 5). Segawa et al. reported a DSSC based on the charge-transfer complex of tetracyanoquinodimethane derivatives with TiO_2 [56]. They pointed out that the charge-transfer complex was formed by the nucleophilic addition of hydroxyl groups on TiO_2 to TCQ moieties. In addition, Houlding and Grätzel reported that 8-hydroxyquinoline was chemically absorbed onto anatase TiO_2 to give a broad absorption spectrum in the visible region [57]. The peak at around 475 nm in the IPCE

Table 3
The effect of dying concentration upon photovoltaic performance of **SQ2-TCAQH**-based DSSCs[a]

Dye conc. (μM)	J_{sc}/mA cm^{-2}	V_{oc}/V	Fill factor	η/%
120	2.51	0.40	0.55	0.55
60	2.78	0.41	0.62	0.71
30	2.89	0.43	0.63	0.78
15	4.33	0.47	0.65	1.31
10	3.48	0.45	0.62	0.97

[a] Conditions: irradiated light, AM 1.5 (100 mW cm^{-2}); dying condition, in acetonitrile/*t*-BuOH at 80 °C without CDCA.

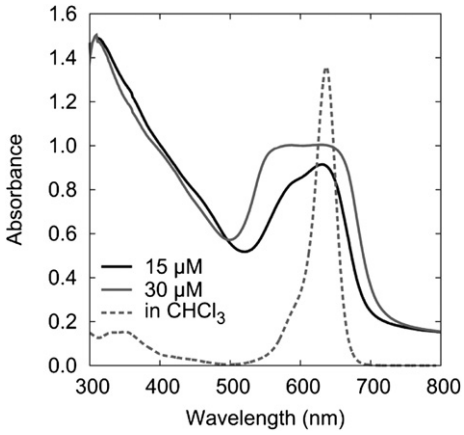

Fig. 4. Absorption spectra of **SQ2-TCAQH** adsorbed on a TiO_2 film at various dyeing concentrations: 15 μM (solid) and 30 μM(gray).

spectrum of **SQ2-TCAQH**-based DSSC might originate from these chemical species on TiO_2 derived from the TCAQ component. The J_{sc} value was significantly improved as a result of the photosensitizing effect at the TCAQ component. The conversion efficiency η was improved in response to an increase in the J_{sc} value, although V_{oc} was somewhat reduced by the change in dyeing conditions. Furthermore, **SQ2-TCAQH**-based DSSC prepared by pretreating the TiO_2 photoelectrode with triethylamine and then thoroughly rinsing the triethylamine away exhibited the highest J_{sc} and η values (Fig. 6, Table 4). In the action spectra, the IPCEs of 600–700 nm originating from the squarylium components were enhanced significantly. Thus, the photovoltaic performance of the DSSC with **SQ2-TCAQH** showed two independent contributions from the TCAQ chromophore and squarylium chromophore. DSSCs prepared with **SQ1-TCQ** and **SQ1-TCAQ** as sensitizers and CDCA as coadsorbent exhibited low performance due to quite low loading of dyes on TiO_2 caused by the lack of hydroxyl groups. In the CDCA-free condition, however, these dyes can moderately adsorb on TiO_2 surface. Absorption of squarylium components increased with increasing the dyeing concentration, although TiO_2 films treated with the 15 μM solution of **SQ1-TCQ** or **SQ1-TCAQ** exhibited little absorption in the far-red region (Fig. 7). Unlike the results of **SQ2-TCAQH**, which showed absorption arising from the aggregation on TiO_2 in the 30 μM condition as shown in Fig. 4, absorption indicating the aggregation of **SQ1-TCQ** and **SQ1-TCAQ** was slightly observed in the 60 μM condition. The photovoltaic performances of

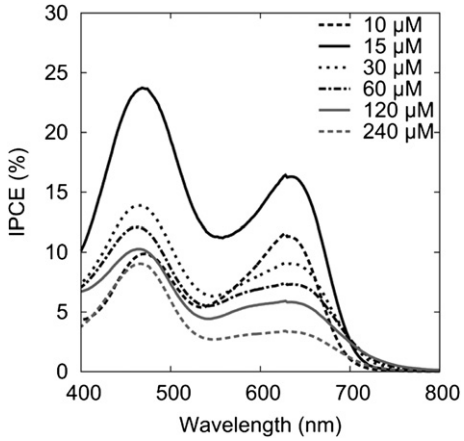

Fig. 5. IPCE for **SQ2-TCAQH**-based DSSCs dyed in various dye concentration without CDCA as a coadsorbent.

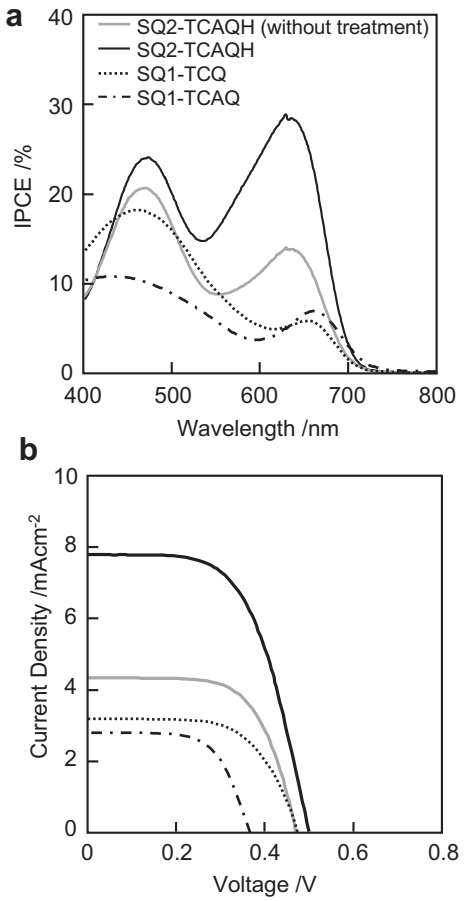

Fig. 6. IPCE spectra (a) and *J*–*V* curves (b) obtained with DSSCs based on **SQ2-TCAQH** (solid), **SQ1-TCQ** (dotted), and **SQ1-TCAQ** (broken) with the pretreated TiO_2 photoelectrode.

cells dyed with **SQ1-TCQ** and **SQ1-TCAQ** in the CDCA-free condition were improved compared with DSSCs containing CDCA with increase in the adsorbed amount (Table 4, Fig. 6). The efficiencies of **SQ1-TCQ** and **SQ1-TCAQ** increased up to 1.03% and 0.67%, respectively. In their IPCE spectra, peaks originated from the contribution of the TCQ or TCAQ chromophore were observed in addition to the squarylium chromophore. However, IPCE values in far-red region were relatively low compared to those at ca. 475 nm. These results indicated that TCQ and TCAQ components are involved in adsorption of dyes on the TiO_2 surface and independently contribute to photoelectric conversion. Meanwhile, the DSSC prepared with **SQ2-TCAQH** in the CDCA-free condition have IPCE maximum at the absorption region of the squarylium component. This result indicates that two chemical species on the TiO_2 surface such as the dye anchored by the hydroxyl group and anchored through the

Table 4
Photovoltaic performance of squarylium-based DSSCs prepared in CDCA-free condition.[a,b]

Dyes	Dye conc. (μM)	J_{sc}/mA cm^{-2}	V_{oc}/V	Fill factor	η/%
SQ2-TCAQH	15	7.77	0.50	0.59	2.29
SQ1-TCQ	15	3.51	0.47	0.63	1.03
SQ1-TCQ	60	3.18	0.48	0.63	0.95
SQ1-TCAQ	15	2.12	0.43	0.60	0.55
SQ1-TCAQ	60	2.81	0.37	0.64	0.67

[a] Conditions: irradiated light, AM 1.5 (100 mW cm^{-2}).
[b] Using a TiO_2 photoelectrode pretreated with triethylamine; dying condition, in acetonitrile/*t*-BuOH at 80 °C without CDCA.

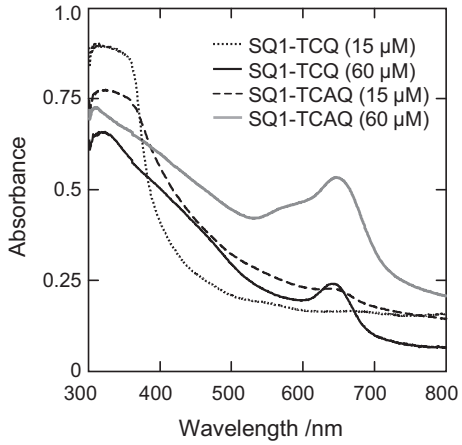

Fig. 7. Absorption spectra of TiO_2 films treated with solutions of **SQ1-TCQ** and **SQ1-TCAQ**.

interaction of TCAQ component with TiO_2 independently contribute the photoelectric conversion.

4. Conclusions

We have demonstrated the design and synthesis of novel squarylium dyes bearing strong electron acceptors as photosensitizers for application to DSSCs. Tetracyanoquinodimethane and tetracyanoanthraquinodimethane moieties with/without hydroxyl groups were used as acceptor components and were incorporated into three squarylium dyes with *N*,*N*-dialkylanilines at the 1,3-position of the cyclobutene core. A nonsymmetrical squarylium dyes, having a *N*,*N*-dialkylaniline and an indolinium moiety on the cyclobutene ring with an ester linking group was also obtained resulting in a total of four squarylium-based diads. The squarylium-based diads exhibited intense absorption bands in the far-red region together with weak absorption bands attributed to acceptor components. The squarylium-based diads having a hydroxyl group were successfully adsorbed on nanocrystalline TiO_2, and DSSCs fabricated from them exhibited a high V_{oc} value (0.66 V), whereas the J_{sc} and η values were still low. These results strongly suggest that the electron-accepting components had effects on the electron injection from the light-harvesting squarylium components to the conduction band of the TiO_2. In the case of the DSSCs prepared without the incorporation of the CDCA, the J_{sc} and η values of photovoltaic cells were improved by the contribution of the photosensitizing effect in the range of wavelength derived from the TCQ and TCAQ chromophore, rather than the squarylium chromophore. This peculiar property implies that TCAQ moieties may act as anchoring units for the TiO_2 surface. Our results suggest that photovoltaic cells using squarylium-based diads showed two independent contributions from the TCAQ chromophore and squarylium chromophore under optimized conditions.

References

[1] Sun S-S, Sariciftci NS. Organic photovoltaics: Mechanisms, materials, and devices. Boca Raton: CRC Press; 2005.
[2] O'Regan B, Grätzel M. A low cost, high-efficiency solar cell based on dye-sensitized colloidal TiO_2 films. Nature 1991;353(6346):737–40.
[3] Hagfeldt A, Grätzel M. Molecular photovoltaics. Accounts of Chemical Research 2000;33(5):269–77.
[4] Nazeeruddine MK, Kay A, Rodicio I, Humphry-Baker R, Müller E, Liska P, et al. Conversion of light to electricity by cis-X2Bis(2,2′-bipyridyl-4,4′-dicarboxylate)ruthenium(II) charge-transfer sensitizers (X = Cl−, Br−, I−, CN−, and SCN−) on nanocrystalline TiO_2 electrodes. Journal of American Chemical Society 1993;115(14):6382–90.

[5] Nazeeruddine MK, Zakeeruddin SM, Humphry-Baker R, Jirousek M, Liska P, Vlachopoulos N, et al. Acid–base equilibria of (2,2′-bipyridyl-4,4′-dicarboxylic acid)ruthenium(II) complexes and the effect of protonation on charge-transfer sensitization of nanocrystalline titania. Inorganic Chemistry 1999;38(26): 6298–305.
[6] Nazeeruddine MK, Péchy P, Grätzel M. Efficient panchromatic sensitization of nanocrystalline TiO_2 films by a black dye based on a trithiocyanato–ruthenium complex. Chemical Communications 1997;18:1705–6.
[7] Chiba Y, Islam A, Watanabe Y, Komiya R, Koide N, Han L. Dye-sensitized solar cells with conversion efficiency of 11.1%. Japanese Journal of Applied Physics Part 2-Letter & Express Letters 2006;45(15):L638–40.
[8] Mishra A, Fischer MKR, Bäuerle P. Metal-free organic dyes for dye-sensitized solar cells: from structure: property relationships to design rules. Angewandte Chemie International Edition 2009;48(14):2474–99.
[9] Wang ZS, Cui Y, Hara K, Dan-oh Y, Kasada C, Shinpo AA. High-light-harvesting-efficiency coumarin dye for stable dye-sensitized solar cells. Advanced Materials 2007;19(8):1138–41.
[10] Hara K, Wang ZS, Sato T, Furube A, Katoh R, Sugihara H, et al. Oligothiophene-containing coumarin dyes for efficient dye-sensitized solar cells. Journal of Physical Chemistry B 2005;109(32):15476–82.
[11] Horiuchi T, Miura H, Sumioka K, Uchida S. High efficiency of dye-sensitized solar cells based on metal-free indoline dyes. Journal of American Chemical Society 2004;126(39):12218–9.
[12] Ito S, Miura H, Uchida S, Takata M, Sumioka K, Liska P, et al. High-conversion-efficiency organic dye-sensitized solar cells with a novel indoline dye. Chemical Communications 2008;(41):5194–6.
[13] Matsui M, Ito A, Kotani M, Kubota Y, Funabiki K, Jin J, et al. The use of indoline dyes in a zinc oxide dye-sensitized solar cell. Dyes and Pigments 2009;80 (2):233–8.
[14] Matsui M, Fujita T, Kubota Y, Funabiki K, Jin J, Yoshida T, et al. Substituent effects in a double rhodanine indoline dye on performance of zinc oxide dye-sensitized solar cell. Dyes and Pigments 2010;86(2):143–8.
[15] Ma X, Hua J, Wu W, Jin Y, Meng F, Zhan W, et al. A high-efficiency cyanine dye for dye-sensitized solar cells. Tetrahedron 2008;64(2):345–50.
[16] Otsuka A, Funabiki K, Sugiyama N, Mase H, Yoshida T, Minoura H, et al. Design and synthesis of near-infrared-active heptamethine–cyanine dyes to suppress aggregation in a dye-sensitized porous zinc oxide solar cell. Chemistry Letters 2008;37(2):176–7.
[17] Chen YS, Li C, Zeng ZH, Wang WB, Wang XS, Zhang BW. Efficient electron injection due to a special adsorbing group's combination of carboxyl and hydroxyl: dye-sensitized solar cells based on new hemicyanine dyes. Journal of Materials Chemistry 2005;15(16):1654–61.
[18] Velusamy M, Thomas KRJ, Lin JT, Hsu YC, Ho KC. Organic dyes incorporating low-band-gap chromophores for dye-sensitized solar cells. Organic Letters 2005;7(10):1899–902.
[19] Chen R, Yang X, Tian H, Wang X, Hagfeldt A, Sun L. Effect of tetrahyroquinoline dyes structure on the performance of organic dye-sensitized solar cells. Chemstry of Materials 2007;19(16):4007–15.
[20] Wang ZS, Koumura N, Cui Y, Takahashi M, Sekiguchi H, Mori A, et al. Hexylthiophene-functionalized carbazole dyes for efficient molecular photovoltaics: tuning of solar-cell performance by structural modification. Chemistry of Materials 2008;20(12):3993–4003.
[21] Tan S, Zhai J, Fang H, Jiu T, Ge J, Li Y, Jiang L, et al. Novel carboxylated oligothiophenes as sensitizers in photoelectric conversion systems. Chemistry-A European Journal 2005;11(21):6272–6.
[22] Tsai MS, Hsu YC, Lin JT, Chen HC, Hsu CP. Organic dyes containing 1*H*-phenanthro[9,10-*d*]imidazole conjugation for solar cells. Journal of Physical Chemistry C 2007;111(50):18785–93.
[23] Yagi S, Nakazumi H. Squarylium dyes and related compounds. Topics in Heterocyclic Chemistry 2008;14:133–81.
[24] Chenthamarakshan CR, Ajayaghosh A. Enhanced sensitivity and selectivity in lithium ion recognition property of an oligomeric squaraine dye based fluorescent sensor. Tetrahedron Letters 1998;39(13):1795–8.
[25] Kim SH, Han SK, Park SH, Lee SM, Lee SM, Koh KN, et al. Use of squarylium dyes as a sensing molecule in optical sensors for the detection of metal ions. Dyes and Pigments 1999;41(3):221–6.
[26] Rou-Lis JV, Martinez-Manez R, Rurack K, Sancenon F, Soto J, Spieles M. Highly selective chromogenic signaling of Hg^{2+} in aqueous media at nanomolar levels employing a squaraine-based reporter. Inorganic Chemistry 2004;43 (17):5183–5.
[27] Arunkumar E, Ajayaghosh A, Daub J. Selective calsium ion sensing with a bichromophoric squaraine foldermer. Journal of the American Chemical Society 2005;127(9):3156–64.
[28] Rou-Lis JV, Marcos MD, Martinez-Manez R, Rurack K, Soto J. A regenerative chemodosimeter based on metal-induced dye formation for the highly selective and sensitive optical determination of Hg^{2+} ions. Angewante Chemie International Edition 2005;44(28):4405–7.
[29] Yagi S, Hyodo Y, Hirose M, Nakazumi H, Sakurai Y, Ajayaghosh A. Metallo supramolecular assemblies of bis-squaraines by callosteric Ca^{2+} ion binding. Organic Letters 2007;9(10):1999–2002.
[30] Welder F, Paul B, Nakazumi H, Yagi S, Colyer CL. Symmetric and asymmetric squarylium dyes as noncovalent protein labels: a study by fluorimetry and capillary electrophoresis. Journal of Chromatography B 2003;793(1):93–105.
[31] Nakazumi H, Colyer CL, Kaihara K, Yagi S, Hyodo Y. Red luminescent squarylium dyes for noncovalent HAS labeling. Chemistry Letters 2003;32 (9):804–5.
[32] Yan WY, Sloat AL, Yagi S, Nakazumi H, Colyer CL. Protein labeling with red squarylium dyes for analysis by capillary electrophoresis with laser-induced fluorescence detection. Electrophoresis 2006;27(7):1347–54.
[33] Jisha VS, Arun KT, Hariharan M, Ramaiah D. Site-selective binding and dual mode recognition of serum albumin by a squaraine dye. Journal of the American Chemical Society 2006;128(18):6024–5.
[34] Matsui M, Tanaka S, Funabiki K, Kitaguchi T. Synthesis, properties, and application as emitters in organic electroluminescence devices of quinacridone- and squarylium-dye-centred dendrimers. Bulletin of the Chemical Society of Japan 2006;79(1):170–6.
[35] Mori T, Kin HG, Mizutani T, Lee DC. Electroluminescent properties in organic light-emitting diode doped with two guest dyes. Japanese Journal of Applied Physics 2001;40(9A):5346–9.
[36] Kim SH, Han SK, Park SH, Park LS. A new dithiosquarylium dye for use as an electron transport material in an organic electroluminescent device having poly (p-phenylene vinylene) as an emitter. Dyes and Pigments 1998;38(1–3):49–56.
[37] Fu N, Baumes JM, Arunkumar E, Noll BC, Smith BD. Squaraine rotaxanes with boat conformation macrocycles. Journal of Organic Chemistry 2009;74(17):6462–8.
[38] Ajayaghosh A, Chithra P, Varghese R. Self-assembly of tripodal squaraines: cation-assisted expression of molecular chirality and change from spherical to helical morphology. Angewandte Chemie International Edition 2007;46 (1–2):230–3.
[39] Mayerhöffer U, Deing K, Gruß K, Braunschweig H, Meerholz K, Würthner F. Outstanding short-circuit currents in BHJ solar cells based on NIR-absorbing acceptor-substituted squaraines. Angewandte Chemie International Edition 2009;48(46):8776–9.
[40] Silvestri F, López-Duarte I, Seitz W, Beverina L, Martínez-Díaz M, Marks T, et al. A squaraine–phthalocyanine ensemble: towards molecular panchromatic sensitizers in solar cells. Chemical Communications 2009;(14):4500–2.
[41] Zhao W, Hou YJ, Wang XS, Zhang BW, Cao Y, Yang R, et al. Study on squarylium cyanine dyes for photoelectric conversion. Solar Energy Materials & Solar Cells 1999;58(2):173–83.
[42] Alex S, Santhosh U, Das S. Dye sensitization of nanocrystalline TiO_2: enhanced efficiency of unsymmetrical versus symmetrical squarain dyes. Journal of Photochemistry and Photobiology A: Chemistry 2005;172(1):63–71.
[43] Chao Li, Wang W, Wang X, Zhang B, Cao Y. Molecular design of squaraine dyes for efficient far-red and near-IR sensitization of solar cells. Chemistry Letters 2005;34(4):554–5.
[44] Chen Y, Zeng Z, Li C, Wang W, Wang X, Zhang B. Highly efficient co-sensitization of nanocrystalline TiO_2 electrodes with plural organic dyes. New Journal of Chemistry 2005;29(6):773–6.
[45] Otsuka A, Funabiki K, Sugiyama N, Yoshida T, Minoura H, Matsui M. Dye sensitization of ZnO by unsymmetrical squaraine dyes suppressing aggrecation. Chemistry Letters 2006;35(6):666–7.
[46] Burke A, Schmidt-Mende L, Ito S, Grätzel M. A novel blue dye for near-IR 'dye-sensitized' solar cell applications. Chemical Communication 2007;(3):234–6.
[47] Yum JH, Walter P, Huber S, Rentsch D, Geiger T, Nüesch F, et al. Efficient far red sensitization of nanocrystalline TiO_2 films by an unsymmetrical squaraine dye. Journal of the American Chemical Society 2007;129(34):10320–1.
[48] Arunkumar E, Chithra P, Ajayaghosh A. A controlled supramolecular approach toward cation-specific chemosensors: alkaline earth metal ion-driven exciton signaling in squaraine tethered podands. Journal of the American Chemical Society 2004;126(21):6590–8.
[49] Raymo FM, Giordani S. Digital processing with a three-state molecular switch. Journal of Organic Chemistry 2003;68(11):4158–69.
[50] Baghdadchi J, Panetta CA. Organic metals. Preparation and properties of 7,7,8,8-tetracyano-*p*-quinodimethaneacetic and -propanoic acid. Journal of Organic Chemistry 1983;48(21):3852–4.
[51] Gómez R, Segura JL, Martín N. New chiral binaphthyl building blocks: synthesis of the first optically active tetrathiafulvalene and 11,11,12,12-tetracyano-9,10-anthraquinodimethane dimers. Journal of Organic Chemistry 2000;65(22):7566–74.
[52] Miguel D, Bryce MR, Goldenberg LM, Beeby A, Khodorkovsky V, Shapiro L, et al. Synthesis and intramolecular charge-transfer properties of new tetrathiafulvalene–σ-tetracyanoanthraquinodimethane diad (TTF–σ-TCNAQ) and triad (TTF–σ-TCNAQ–σ-TTF) molecules. J. Mater. Chem. 1998;8(1):71–6.
[53] Hyodo Y, Nakazumi H, Yagi S. Synthesis and light absorption/emission properties of novel squarylium dimmers bearing a ferrocene spacer. Dyes and Pigments 2002;54(2):163–71.
[54] Hagfeldt A, Grätzel M. Light-induced redox reactions in nanocrystalline systems. Chemical Reviews 1995;95(1):49–68.
[55] Hara K, Dan-oh Y, Kasada C, Ohga Y, Shinpo A, Suga S, et al. Effect of additives on the photovoltaic performance of coumarin-dye-sensitized nanocrystalline TiO_2 solar cells. Langmuir 2004;20(10):4205–10.
[56] Fujisawa J, Nagatani T, Sanehira T, Nakazaki J, Uchida S, Kubo T, et al. Novel solar cells based on surface complexes of TiO_2 with dicyanomethylene compounds. National Meeting of the Chemical Society of Japan 2008;89(1):91.
[57] Houlding VH, Grätzel M. Photochemical H_2 generation by visible light. Sensitization of TiO_2 particles by surface complexation with 8-hydroxyquinoline. Journal of the American Chemical Society 1983;105(17):5695–6.